

Alma Mater Studiorum Università di Bologna
Archivio istituzionale della ricerca

L-CSMA: A MAC Protocol for Multihop Linear Wireless (Sensor) Networks

This is the final peer-reviewed author's accepted manuscript (postprint) of the following publication:

Published Version:

Buratti, C., Verdone, R. (2016). L-CSMA: A MAC Protocol for Multihop Linear Wireless (Sensor) Networks. IEEE TRANSACTIONS ON VEHICULAR TECHNOLOGY, 65(1), 251-265 [10.1109/TVT.2015.2391302].

Availability:

This version is available at: <https://hdl.handle.net/11585/598129> since: 2017-06-13

Published:

DOI: <http://doi.org/10.1109/TVT.2015.2391302>

Terms of use:

Some rights reserved. The terms and conditions for the reuse of this version of the manuscript are specified in the publishing policy. For all terms of use and more information see the publisher's website.

This item was downloaded from IRIS Università di Bologna (<https://cris.unibo.it/>).
When citing, please refer to the published version.

(Article begins on next page)

This is the final peer-reviewed accepted manuscript of:

C. Buratti and R. Verdone, "L-CSMA: A MAC Protocol for Multihop Linear Wireless (Sensor) Networks", in IEEE Transactions on Vehicular Technology, vol. 65, no. 1, pp. 251-265, Jan. 2016, doi: 10.1109/TVT.2015.2391302

The final published version is available online at:
<https://doi.org/10.1109/TVT.2015.2391302>

Rights / License:

The terms and conditions for the reuse of this version of the manuscript are specified in the publishing policy. For all terms of use and more information see the publisher's website.

This item was downloaded from IRIS Università di Bologna (<https://cris.unibo.it/>)

When citing, please refer to the published version.

L-CSMA: A MAC Protocol for Multihop Linear Wireless (Sensor) Networks

Chiara Buratti, *Member, IEEE*, and Roberto Verdone, *Member, IEEE*

Abstract—We consider a multihop wireless linear network where multiple nodes are evenly spaced over a straight line. Two scenarios are addressed: a network where only one source generates traffic to be transmitted via multiple hops to the destination and the case of linear sensor networks where all nodes in the line generate data. A novel contention-based medium access control (MAC) protocol, called L-CSMA, specifically devised for linear topologies, is proposed. Carrier-sensing multiple access (CSMA) suffers from the well-known hidden/exposed-node problems: The scope of L-CSMA is to reduce their impact, while minimizing the protocol overhead. L-CSMA assigns different levels of priority to nodes, depending on their positions in the line: Nodes closer to the destination have higher priority when accessing the channel. The priority is managed by assigning to nodes different durations of the carrier-sensing phase. This mechanism speeds up the transmission of packets that are already in the path, making the transmission flow more efficient. Results show that L-CSMA outperforms existing contention-based MAC protocols. A mathematical model to derive the performance in terms of packet success probability and throughput is provided. The key idea of the model is the definition of the generic state at the network level, instead of the node level, and its representation through a set of bits indicating the status (activity or not) of the corresponding link. The model is validated through comparison with simulations.

Index Terms—CSMA, linear networks, MAC protocols, mathematical modelling, multihop, wireless sensor networks.

I. INTRODUCTION

LINEAR wireless networks (LWNs), where nodes are regularly deployed over a straight line and data transmission happens hop by hop through all nodes, are increasingly attracting interest [1], [2]. Generally, in these applications, data are generated by a source node in the line, which has to transmit it toward a given destination node in the line, passing through some relays. The specific case of linear wireless sensor networks (LWSNs) is perhaps the most relevant, with applications, for example, in the area of gas/water/oil pipeline control [3], river environmental monitoring [4], and smart cities where sensors are regularly deployed on the asphalt or on the lamp posts

[5]. In the case of LWSNs, all nodes generate data to be transmitted toward a specific destination node (the sink). In this paper, we denote as *LWN* a network where only the first node in the line acts as a source generating data for a destination node at the end of the line, with relays in between the two extremes, and as *LWSN* a network where all nodes (but the destination) generate data (both the source and relays).

While in general the medium access control (MAC) and routing protocols represent the most delicate components of the protocol stack in multihop networks, in the case of linear and regular topologies, the routing mechanisms can be simplified, owing to the network geometry. Therefore, we focus on the MAC layer. We assume that when the MAC algorithm runs in a wireless node to access the radio channel, the routing protocol at the upper layer has already set the complete route (i.e., each node knows the next hop); each node is aware of the number of relays in the path toward the destination (as usual, in routing protocols such as, e.g., ad hoc on demand distance vector).

In most of the application examples previously mentioned, owing to the possible presence of long sequences of nodes, there is no centralized network control; therefore, contention-free scheduling of transmissions is difficult to achieve. As usual, in this case, the class of carrier-sensing multiple access (CSMA)-based protocols is considered, with nodes sensing the channel to assess whether it is busy or free (as in the IEEE 802.11 or 802.15.4 families of protocols). CSMA is known to suffer from the hidden/exposed-node problems [6]: The former consists of the fact that carrier-sensing is made at the transmitter side, and even if no transmissions are detected, some active interfering node might be close to the receiver while hidden to the transmitter, causing packet collision and loss; a well-known solution is represented by the request-to-send (RTS)/clear-to-send (CTS) mechanism [7], which, however, introduces protocol overhead and generates the exposed-node problem (with a node inhibited by a transmitter sending the RTS, even if far from its receiver).

In this paper, we propose a CSMA-based protocol, which is called L-CSMA, specifically devised for linear networks; it reduces the impact of the hidden-terminal problem, without the use of RTS/CTS packets, therefore preventing the increase of the exposed-node problem. L-CSMA assigns different levels of priority to nodes when accessing the channel, depending on their positions in the line: Nodes closer to the destination have higher priority. The priority is managed by assigning to nodes different durations of the carrier-sensing phase; nodes closer to the destination sense the radio channel for a shorter time. While this mechanism has been proposed in other papers to allow the

This work was supported by the European Commission in the framework of the FP7 Network of Excellence in Wireless COMMunications (NEWCOM#) under Grant 318306. The review of this paper was coordinated by Prof. X. Wang.

The authors are with the Department of Electrical, Electronic and Information Engineering (DEI), University of Bologna, 40136 Bologna, Italy (e-mail: c.buratti@unibo.it; roberto.verdone@unibo.it).

management of different priority levels of data packets [8]–[11], here, it is used to speed up the transmission of packets that are already in the path, making the transmission flow more efficient: The proposed protocol allows to avoid starvation of packets at intermediate relays.

L-CSMA can be applied both to LWNs and LWSNs, provided that relay nodes append the data they locally generate to the payload of the packet they have just received from the previous hop (the simplest form of data aggregation or data concatenation [12]); therefore, packets generated by the source, which flow through the line, act as tokens, giving the right to nodes to transmit their data. It is shown that the protocol proposed inherently allows the efficient transmission of the multiple data blocks; in fact, at each hop, the carrier-sensing phase is made shorter, thus leaving more room for data transmission within the slot duration. L-CSMA is designed such that, under ideal channel conditions (i.e., no fading), packet collisions are completely avoided, by properly setting the sensing threshold. To measure its performance in more undetermined environments, we consider the presence of fading, which causes packet collisions. A power control mechanism is applied to limit the amount of packet losses.

A mathematical model for evaluating the network performance of L-CSMA is also introduced in the paper. It is based on a novel approach using state transition diagram analysis, where states are defined according to the transmissions occurring within each hop and on the state of the queue at nodes. The novelty of the approach stands in the fact that the generic state represents the network status, instead of the node status, as largely done in the literature (see, e.g., [13]–[15]). Since the model includes some simplifying approximations, it is validated through simulations. A very good fit is found, showing that it captures the essential elements of the protocol.

Summing up, the main contributions of this paper are

- the proposal of a novel MAC protocol for multihop LWNs or LWSNs, based on CSMA;
- the proposal of a mathematical model for the L-CSMA protocol, based on a novel approach.

The rest of this paper is organized as follows. The following section discusses related works and the scope of this paper. Section III introduces the reference scenario and assumptions. Section IV describes L-CSMA. In Section V, the mathematical model is described. In Section VI, the benchmark protocols are introduced; numerical results are discussed and the model is validated in Section VII. The final section summarizes the main contributions of this paper.

II. RELATED WORKS AND SCOPE OF THIS PAPER

A. Literature Survey

Many works in the literature study the performance of contention-based protocols for wireless networks. ALOHA, presented by Abramson in 1970 in [16], was one of the first MAC protocols for radio networks. Later, both theoretical and practical studies have been carried out to improve ALOHA; we mention as an example the work by Roberts [17] on slotted ALOHA. A 2-D Poisson distributed network is considered in

[18], where the performance of both, i.e., ALOHA and CSMA, are studied. In [19], the success probability of ALOHA and CSMA is studied, assuming an interference-free guard zone around the receiver. However, the abovementioned works focused on a single-hop scenario.

The first paper studying ALOHA in a multihop context is [20], where the probability of successful transmission is evaluated, considering a simple model where interference only propagates two hops away. In [21], a widely accepted model for ALOHA in a network with spatial reuse was introduced. In [22], the problem of starvation and throughput imbalances in multihop CSMA-based wireless networks is addressed. In [23], the use of CSMA with collision avoidance (CSMA/CA) protocols in multihop wireless networks is studied, and [24] shows the performance of a CSMA protocol in a 2-D Poisson distributed multihop network. In [25], nodes distributed according to a Poisson point process over a line are considered, and the performance of a CSMA-based protocol is evaluated. Finally, in [26]–[28], networks with an infinite number of nodes are considered. In contrast with the latter works, we propose a mathematical model for a multihop network with a finite number of nodes.

Priority issues have been largely studied in IEEE 802.11 networks (see, e.g., [8], [11], and [29]). As an example, reference [11] proposes a token passing-based MAC protocol to be used to manage real-time traffic in 802.11 networks. A virtual token circulates among real-time-constrained devices with the aim of prioritizing real-time traffic. However, IEEE 802.11 is not suitable for wireless sensor networks; therefore, it is not considered in this paper. Many works are also dealing with the proposal of priority schemes to be applied to IEEE 802.15.4, all with the objective to provide different priority levels to data packets, that is to guarantee different quality-of-service levels: reference [9] proposes to adapt the sleeping period duration depending on the priority level; in [10], a priority-based service differentiation scheme is presented; reference [30] extends the 802.15.4 standard to prioritize packet delivery time, whereas in [31], an efficient utilization-aware guaranteed time slot allocation scheme to enhance quality of service is proposed. In contrast with the aforementioned works, where the priority concept is applied to packets to get different quality-of-service levels, in this work, the priority concept is applied to nodes, with the aim of reducing the hidden-terminal problem and increasing the throughput.

While most papers dedicated to wireless multihop networks consider bidimensional scenarios [26], [27], [32], several works in the literature also propose and study MAC protocols for linear topologies. In [33], ALOHA and CSMA/CA protocols, when considering a linear and a grid topology, are compared in terms of throughput. In [34], routing schemes for LWNs are proposed, where a source node transmits data to a destination node, and intermediate nodes are equidistantly placed on a line. In [35], the threshold phenomena and the MAC-layer capacity in finite wireless networks on a line, using random geometric graphs, are studied. Finally, in [36] a token passing mechanism is proposed, using RTS/CTS plus a novel control packet, which is called ready-to-receive (RTR), to manage the flow of data in the line. While these control packets reduce the hidden-terminal

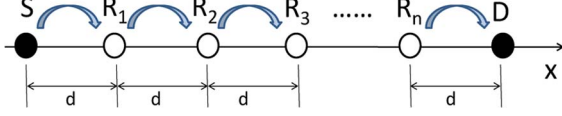


Fig. 1. Linear network.

problem and keep under control losses, they cause a decrease in the network throughput, generating overhead and the exposed-terminal problem. Results shown in this paper demonstrate that L-CSMA performs better than Ripple [36].

B. Scope of This Paper

In this paper, the linear topology is regular, with a finite number of nodes, evenly distributed over the line; this is motivated by most of the real reference applications for linear networks (see, e.g., [5]). The idea of providing higher priority in the access to nodes closer to the destination is analyzed and compared with IEEE 802.15.4 [37], slotted ALOHA [16], and Ripple [36]. L-CSMA is shown to outperform the other solutions. This paper is inspired by a previous work, i.e., [38], having similar objectives but not considering: 1) the LWSN case; 2) power control and implicit acknowledgement; 3) the queue status in the mathematical model; and 4) random channel fluctuations. Moreover, in [38], a simplified packet capture model (hop-based) is considered.

III. REFERENCE SCENARIO AND ASSUMPTIONS

The reference scenario is shown in Fig. 1: The source (S) and the destination node (D) are separated by n relays R_1, \dots, R_n . Nodes are evenly spaced over the line, with a distance d between each pair of consecutive nodes. We assume that the routing algorithm has established a route where each node forwards the packet to that next in line. The number of hops from S to D, which is denoted as z hereafter, is therefore $z = n + 1$.

We assume that nodes are time synchronized (at the level of packet frame only): Time axis is divided into slots of duration T_{slot} [s]. This does not require network centralization, as distributed synchronization schemes can be run at the expense of minimum overhead [39].

We assume that the source is ready to generate a new packet at each slot. However, depending on the MAC protocol and the overall network status, S could sometimes be inhibited in the transmission of a new packet.

A. Assumptions: Channel and Packet Capture Models

In this paper, we model the power loss due to propagation effects including a distance-dependent path loss and fast channel fluctuations. We assume that the received power, denoted as P_R , depends on the transmit power, denoted as P_T , according to the following expression:

$$P_R = P_T \cdot k \cdot x^{-\beta} \cdot f \quad (1)$$

where k is a constant, x is the distance between the nodes considered, β is the attenuation coefficient, and finally, f is the short-term (fast) random fading component. Rayleigh fading

is assumed; therefore, f is negative exponentially distributed (with unit mean). We also assume the following.

- 1) A transmitter and a receiver can communicate if $P_R \geq P_{R_{\min}}$, being $P_{R_{\min}}$ the receiver sensitivity.
- 2) A node can “hear” a transmitter during carrier-sensing if $P_R \geq P_{S_{\min}}$, where $P_{S_{\min}}$ is the sensing threshold (normally smaller than receiver sensitivity).
- 3) A packet is captured by a receiver if condition 1) is satisfied and if the ratio between the useful and the interfering power, denoted as C/I , is larger or equal to the capture threshold, denoted as α .

C of condition 3 is the useful received power, equal to P_R with $x = d$, whereas I is the sum of all interfering power; however, in the mathematical model, I is approximated with the power received from the nearest interferer (see Section V).¹ A comparison with simulation results demonstrates that, owing to the linearity of the topology, the impact of this simplifying assumption is not very significant (see Section VII). See [40] for more details about the implemented capture effect model.

Owing to the presence of fading, each of the given three conditions is subject to randomness for each pair of nodes in the line.

We assume that all links are independent and symmetric and that link-level-based power control is applied. Therefore, the given first condition is satisfied by all pairs of consecutive nodes in the line with probability 1, that is the network is fully connected. According to power control, the transmit power at node i is set as follows:

$$P_T^{(i)} = \frac{P_{R_{\min}} d^{\beta}}{k f_{i,i+1}} \quad (2)$$

where $f_{i,i+1}$ is the short-term fading sample when node i is transmitting and node $i + 1$ is receiving, with $i \in \{0, \dots, n\}$.

Finally, we assume that the channel coherence time is much larger than the average time needed for the transmission of one packet from S to D.

B. LWN Scenario

We first consider a multihop LWN where the source generates data blocks to be transmitted to the destination node via the n relays. The source generates a packet composed of a header (H bits) and a payload (P bits); we denote as $Z = H + P$ the overall number of bits in the packet, which is transmitted at bit rate R_b . The packet is then forwarded by the relays toward the destination, that is all nodes transmit a packet of the same size, Z . By denoting as $T_p^{(i)}$ the packet length sent by the (i) th node, where $i = 0$ indicates the source, and $i \in \{1, \dots, n\}$ refers to the n relays, we have $T_p^{(i)} = Z/R_b$ for $i \in \{0, \dots, n\}$.

C. LWSN Scenario

In the case of an LWSN, all nodes (but the destination) have data to transmit. We assume that at each slot, every node can sample the environment and generate P bits of data.

¹Owing to the linearity of the regular topology, the nearest interferer will also be the strongest with very high probability, even in the presence of fading.

However, the nodes actually sample, elaborate the data, and generate the data block only when they are allowed to transmit (according to L-CSMA) to avoid useless consumption of energy and computing resources. In particular, sensor nodes in the line are allowed to send their data only after they receive a packet from the previous node in the line, acting as token.

When a node is allowed to transmit in one slot, it generates and appends the P bits to the payload of the last packet received from the previous node in the line (a simple form of data aggregation); as a result, the packet will be longer. In this case, the packet length is given by $T_p^{(i+1)} = T_p^{(i)} + P/R_b$, where $T_p^{(0)} = Z/R_b$. T_{slot} is larger than $T_p^{(n)}$, i.e., than the longest packet (see below).

IV. L-CARRIER SENSING MULTIPLE ACCESS PROTOCOL

The basic idea behind L-CSMA starts from the observation that, with traditional CSMA protocols, when a source node has many packets to send over an established route, they compete for accessing the radio channel with those that were previously transmitted and are still being forwarded by some relays in the route. More generally, a packet to be sent by a node in the route to the next relay will compete for access with both those packets that are to be transmitted by nodes forward in the line and those in the rear.

To take advantage of the linear topology and to avoid congestion of data blocks at relays, we assign to nodes in the route different levels of priority in the access to the channel: Nodes closer to the destination have higher priority with respect to those closer to the source. To simply implement the different levels of priority, we impose that nodes sense the channel for different intervals of time: The shorter the sensing duration, the higher the priority in the access to the channel. Once the node knows the number of hops to reach the source (i.e., its position in the hop sequence with respect to the source), the node will select the proper sensing duration. The latter brings 1) reduction of the hidden-terminal problem, preventing collisions with packets that are in the rear; and 2) reduction of the exposed-terminal problem, preventing inhibition caused by nodes forward in the line.

We measure 1) the source success probability p_S , which is the probability that a packet generated by the source is correctly received by the destination; 2) the average success probability \bar{p}_S , which is the probability that a packet generated by a node is correctly received by D, averaged among nodes (evaluated in the case of LWSN); 3) the normalized source throughput $\hat{\Sigma}$, which is defined as the average number of packets generated by the source and correctly received by D per slot (whose maximum value is 1); and 4) the source throughput Σ which is defined as the number of information bits per second generated by the source and correctly received by D.

If a packet were generated by the source every $n + 1$ slots, only one packet at a time would be transmitted in each slot in the network, ensuring that no packet collisions would happen. The system (under ideal channel conditions and perfect connectivity) would give $p_S = 1$ and $\hat{\Sigma} = 1/(n + 1)$. The goal of L-CSMA is to increase the normalized throughput by allowing

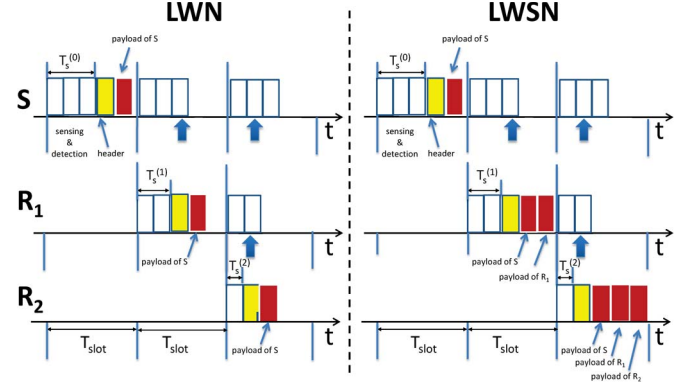


Fig. 2. Access to the channel in the case of a three-hop network composed of nodes S, R_1 , R_2 , and D. An example.

concurrent transmissions of separate packets in the line (a goal that requires control of the packet success probability).

A. LWN Protocol

To proceed with the protocol description, let us first consider the LWN case, with one single source of traffic in the line, namely, node S.

Each slot is split into three parts for all nodes (see Fig. 2).

- First part: The transmitter senses the radio channel for an interval $T_s^{(i)}$, where $i \in \{0, \dots, n\}$; we set $T_s^{(i)} = (n - i + 1) \cdot T$, where T (the minimum sensing duration, which is applied by the last relay in the line, $i = n$) is set equal to P/R_b , that is the time needed to transmit the payload.²
- Second part: If the channel was sensed free, the packet is transmitted to the next node in the line (otherwise, the node switches to receiver mode). Since only the source is generating data, the transmission time is $T_p^{(i)} = Z/R_b$ for each node.
- Third part: A guard time (whose duration is $T_g^{(i)} = i \cdot T$) between the end of the packet and the beginning of the subsequent slot is kept.

Therefore, $T_{slot} = T_s^{(i)} + T_p^{(i)} + T_g^{(i)} = (n + 2) \cdot T + H/R_b$.

According to this, any node X (e.g., the second relay) that can be heard by a given node Y (e.g., the source) that is behind in the line will access the radio channel before Y ends the sensing phase; node Y will then hear the transmission by X , presume a harmful interference at the receiving side (the first relay), and defer any other activity to the next slot. Assuming ideal channel conditions, this prevents having collisions from packets that are in the rear; on the other hand, transmission happens at a node only if the previous packet in the flow is sufficiently ahead in the line, which is a condition that prevents from harmful interference from the nodes that are further in the line.

Therefore, the advantage of providing priority to those packets in the route that are closer to the destination stands in the fact

²The minimum amount of time needed for efficient sensing of the radio channel in CSMA standards is normally compatible with this assumption, provided that P is not too large.

that they will not compete with those transmitted in the rear. This mechanism speeds up the transmission of packets that are already in the route. On the other hand, this protocol requires longer sensing times, which erode the amount of radio resource used for the transmission of useful information. In the performance analysis, we carry out accounts for both effects.

B. LWSN Protocol

Fig. 2 (right part) shows the protocol behavior in the case of an LWSN with three hops ($z = 3$). In the case of LWSN, the sensing durations, denoted as $T_s^{(i)}$, are the same set for the case of LWNs. Therefore, the source node will sense the channel for a longer time than relays; however, the latter transmit longer packets (that includes multiple data blocks) and the two effects are complementary. The latter is given by $T_p^{(i)} = T_p^{(0)} + i \cdot P/R_b$. As a result, the guard time is set to zero in all hops (i.e., $T_g^{(i)} = 0$). Any other aspect of the protocol is similar to the case of the LWN, bringing to a condition where no collisions can happen if the radio channel is deterministic. Moreover, the slot duration is still given by $T_{\text{slot}} = T_s^{(i)} + T_p^{(i)} = (n+2) \cdot T + H/R_b$.

C. Countermeasures to Fading

In the presence of fading, connectivity issues between two consecutive nodes in the line can happen, causing losses of packets because of disconnected link(s).

To overcome the given issue, we apply power control, which is implemented by introducing an implicit-acknowledge mechanism as follows. After the transmission of a packet by node R_i toward node R_{i+1} , node R_i will listen to the channel for the following slots, waiting for the reception of the packet that node R_{i+1} is forwarding toward node R_{i+2} . Upon reception of such packet, R_i will get an implicit acknowledgement on its previous transmission.

Moreover, node R_{i+1} will include in the header of the packet the level of transmit power used (one byte is sufficient), such that node R_i can compute the loss between itself and the receiver, i.e., R_{i+1} , and can implement power control for the following transmissions.

The use of power control prevents connectivity issues, but collisions can still happen, because a node X (e.g., the second relay) can be hidden to Y (e.g., the source) owing to a bad channel sample, while its transmission might be characterized by a strong power level at the intended receiver (the third relay). We need then to discuss how the protocol will behave in the presence of collisions and packet losses.

When a node R_i in the line performs its transmission to the next node, i.e., R_{i+1} , there are three different events that can happen.

- 1) The packet is correctly received at the current time slot, and at the next slot, R_{i+1} will try to access the channel, and once successful, its transmission will be heard by R_i (which is in sensing and detection state): This packet will act as an implicit acknowledgement.
- 2) The packet is correctly received by R_{i+1} , but when R_{i+1} will access the channel (with a level of transmit power set

to guarantee $P_R \geq P_{R_{\min}}$ at R_{i+2}), its transmission will not be heard by R_i .

- 3) The packet is lost owing to collisions, and R_{i+1} will generate no implicit acknowledgement.

In the two latter cases, a potential deadlock condition is generated, with R_i waiting for some acknowledgement that will never come. In these cases, a timeout approach is the solution we take, with R_i trying to transmit the next packet W slots after the transmission of the previous packet. W is set to 1 in this paper for the sake of throughput maximization.

Finally, note that in case of a packet loss, it does not make sense to retransmit the packet, as new data can be generated at the next slot. However, for the sake of completeness, the use of retransmissions is also investigated in Section VII.

V. MATHEMATICAL MODEL

We assume perfect power control, that is, each node in the line is able to measure the fading sample to be used for the transmission, according to the procedure previously described. Given the latter, no connectivity issues are present (i.e., condition 1 defined in Section III-A is always satisfied); therefore, losses are only due to possible collisions. In this case, the success probability for the source node, in the case of LWNs, represents the probability that C/I is larger or equal to the capture threshold, in all the links connecting S to D. In the case of LWSNs, we will evaluate the success probability averaged among the nodes (nodes nearer to the destination will have larger success probability with respect to those farther).

As far as throughput is concerned, according to the definitions given in Section III, the source throughput in both LWNs and LWSNs is given by

$$\Sigma = \hat{\Sigma} \cdot \frac{P}{T_{\text{slot}}} \text{ [bit/s]}. \quad (3)$$

Note that for the case of LWSNs, we could also evaluate the network (i.e., generated by all nodes in the network) throughput; however, the latter is simply $\Sigma \cdot (n+1)$, since in LWSNs, a correctly received packet carries the information generated by all the $n+1$ sources. As a result, there is only a scaling factor that would differentiate the two throughput definitions, and for this reason, only results related to Σ defined in (3) are provided.

In the remainder of this section, we first introduce notations and describe formally the sensing mechanism and packet capture; then, we provide the model for the cases: $z = 3, 4$, and 5 (the two-hop case is trivial).

A. Notations

To evaluate p_S , \bar{p}_S , and $\hat{\Sigma}$, we model the network behavior through a finite-state transition diagram [41]. The network status, denoted as $\mathbf{S}^{(z)}$, can be modeled through a $(2 \cdot z)$ -dimensional stochastic binary and stationary process, composed of two sequences of bits, denoted as $\mathbf{S}^{(z)} = \{\mathbf{L}^{(z)}, \mathbf{Q}^{(z)}\}$, where $\mathbf{L}^{(z)} = \{L_0, \dots, L_{z-1}\}$ is a z -bit sequence representing the status of each link in a given slot, connecting R_i to R_{i+1} , with $i \in \{0, \dots, n\}$, whereas the z -dimensional sequence of bits, i.e., $\mathbf{Q}^{(z)} = \{Q_0 \dots Q_{z-1}\}$, represents the status

of the queue of nodes in the route, i.e., of nodes R_i with $i \in \{0, \dots, n\}$, during the same slot. In particular, $L_i = 1$ in case of active link, that is in case during the slot there is a transmission occurring on link i , that is from R_i to R_{i+1} , and $L_i = 0$, otherwise. We set $Q_i = 1$ if node R_i has a packet in the queue, because 1) a new one has been generated, or 2) there is a packet in the queue that was not transmitted because the channel was detected as busy. Note that the “1”s in the vector $\mathbf{L}^{(z)}$ represent packets that are traveling the radio channel and are not in the queue of any nodes during the slot.

We denote as $s^{(z)}$ the number of the possible states in which the z -hop route could be, and as $\pi^{(z)}$ the $s^{(z)}$ -dimensional state probabilities vector, where each element is given by: $\mathbb{P}\{L_0 = l_0, \dots, L_{z-1} = l_{z-1}, Q_0 = q_0, \dots, Q_{z-1} = q_{z-1}\} = \pi_{l_0, \dots, l_{z-1}, q_0, \dots, q_{z-1}}$, also denoted as $\pi_{\mathbf{l}^{(z)}, \mathbf{q}^{(z)}}$, where $\mathbf{l}^{(z)}$ and $\mathbf{q}^{(z)}$ are sequences of z bits. We also denote as $\mathbf{P}^{(z)}$ the $s^{(z)} \times s^{(z)}$ matrix of the state transition probabilities, where $P_{ij}^{(z)}(t) = \mathbb{P}\{\mathbf{S}^{(z)}(t) = \{\mathbf{L}_j^{(z)}, \mathbf{Q}_j^{(z)}\} | \mathbf{S}^{(z)}(t-1) = \{\mathbf{L}_i^{(z)}, \mathbf{Q}_i^{(z)}\}\}$ is the probability of passing from state $\{\mathbf{L}_i^{(z)}, \mathbf{Q}_i^{(z)}\}$ to state $\{\mathbf{L}_j^{(z)}, \mathbf{Q}_j^{(z)}\}$ in t that is equal to $P_{ij}^{(z)}$, i.e., it is independent of time t owing to the stationarity of the process.

Due to the complexity in the evaluation of p_S , \bar{p}_S and $\hat{\Sigma}$, which increases by getting z larger, we report in the following the complete analysis in the cases $z \leq 5$. Simulations are also used to show results achieved with the L-CSMA protocol when $z > 5$. We refer to [40] for the discussion about the possible extension of the model to the case of larger networks.

In the model, the following simplifying assumptions are made: 1) Two consecutive nodes in the line, being connected (due to the power control), can also “hear” each other; 2) only the nearest interferer is considered to evaluate the interfering power (as in [25]); 3) the probabilities $c_{i,j}$ that a packet transmitted by node i and interfered by node j is captured (by node $i+1$) are assumed to be independent, whatever the values of i and j . With reference to assumption 1), it could happen that a node i cannot “hear” node $i+1$, since the transmit power of node $i+1$ is set according to the fading sample between node $i+1$ and $i+2$ and does not depend on $f_{i,i+1}$. However, being $P_{S_{\min}} \leq P_{R_{\min}}$, according to most real devices, the latter event happens with very low probability. For that which concerns assumption 3), if we consider, for example, a three-hop network, we have that c_{02} and c_{13} are correlated since they both depend on the fading sample between R_1 and R_2 , $f_{1,2} = f_{2,1}$.³ However, in the mathematical model, to compute the joint probability (e.g., the probability that the packet sent by S is captured when interfered by R_2 and that the packet sent by R_1 is captured when interfered by R_3), we assume that the two events are independent, and we just multiply the two probabilities, i.e., c_{02} and c_{13} (see below). Comparison with simulation results demonstrates that, owing to the linearity of the topology, the impact of the simplifying assumptions is not very significant. Finally, as previously stated, the model is derived for the case $W = 1$.

B. Sensing and Packet Capture

We denote as $h_{i,j}$ the probability that node i can “hear” node j (and *vice versa*), which is given by

$$h_{i,j} = \mathbb{P}\{P_{R_i}^{(j)} \geq P_{S_{\min}}\} = \mathbb{P}\{P_T^{(j)} k d_{i,j}^{-\beta} f_{j,i} \geq P_{S_{\min}}\}$$

where $P_{R_i}^{(j)}$ is the power received by node i when node j is transmitting, given by (1), $f_{j,i}$ is the fading sample between node j (the transmitter) and node i (the receiver), and $d_{i,j}$ is the distance between nodes i and j , which will be expressed in the following as $x_{i,j} \cdot d$, being $x_{i,j}$ an integer. By using (2) and recalling that the random variable representing fading is negative exponentially distributed, we have

$$\begin{aligned} h_{i,j} &= \mathbb{P}\left\{\frac{f_{j,j+1}}{f_{j,i}} \leq \frac{P_{R_{\min}}}{P_{S_{\min}}} x_{i,j}^{-\beta}\right\} \\ &= \int_0^{+\infty} \int_0^{\gamma} e^{-(f_{j,i} + f_{j,j+1})} df_{j,i} df_{j,j+1} \end{aligned}$$

where $\gamma = (P_{R_{\min}}/P_{S_{\min}})x_{i,j}^{-\beta}$. The latter results in $h(x_{i,j}) \triangleq h_{i,j} = \gamma/(1 + \gamma)$.

For what concerns the capture effect, we have

$$c_{i,j} = \mathbb{P}\left\{\frac{C^{(i)}}{I^{(j)}} \geq \alpha\right\} = \mathbb{P}\left\{\frac{f_{j,i+1}}{f_{j,j+1}} \leq \frac{x_{i+1,j}^{\beta}}{\alpha}\right\}$$

which is obtained by denoting as $x_{i+1,j} \cdot d$ the distance between the interferer j and the useful receiver, $i+1$ and using the following constraints: $C^{(i)} = P_{R_{i+1}}^{(i)} = P_{R_{\min}}$ and $I^{(j)} = P_T^{(j)} k (x_{i+1,j} \cdot d)^{-\beta} f_{j,i+1} = P_{R_{\min}} x_{i+1,j}^{-\beta} (f_{j,i+1}/f_{j,j+1})$.

The latter results in $c(x_{i+1,j}) \triangleq c_{i,j} = \xi/(1 + \xi)$, where $\xi = x_{i+1,j}^{\beta}/\alpha$.

C. Three-Hop Network

In Fig. 3, we show the finite-state transition diagram describing the behavior of the network when two relays are present. In the diagram, h_{02} represents the probability that node zero (the source) and relay 2 can “hear” each other (and $\bar{h}_{02} = 1 - h_{02}$), whereas c_{02} is the probability that the packet transmitted by node zero and interfered by relay 2 is captured (and $\bar{c}_{02} = 1 - c_{02}$).

Each state is represented by two sequences of three bits each, representing the status (active or not) of the first, the second, and the third links, and of the queues of source, R_1 and R_2 , respectively. In particular, the possible states in which a three-hop network can be are $\mathbf{S}^{(3)} = \{\{100,100\}, \{010,100\}, \{001,100\}, \{000,100\}, \{101,100\}\}$.

Note that the diagram has been derived considering an LWN application, where only the source generates data, and its queue has always a data block ready to be transmitted, according to our application. The latter results in having $\mathbf{Q}^{(3)} = \{100\}$ for all the states, since in this particular network, there are no cases in which relays are inhibited in the transmission, and their data blocks remain in the queue for more than one slot. Note that the results related to the LWSNs can be extrapolated from the same diagram, bearing in mind the following: 1) Each relay

³Owing to the symmetry of links.

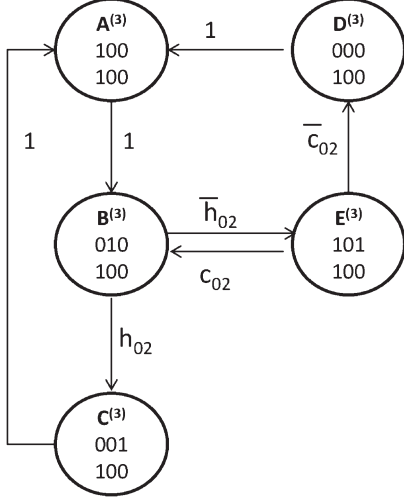


Fig. 3. Finite-state transition diagram for a three-hop network.

generates its own data block when a packet is received from the previous node in the route; 2) when a data block is received by D, it always carries $z = 3$ data packets (i.e., payloads); 3) in the $\mathbf{Q}^{(z)}$ vector, representing the status of the queues, we do not account for data generated at intermediate nodes (but only at the source), since these packets are really included in the queue only when the token is received.

For the sake of readability in the following, we will denote the given states also as (see Fig. 3): $\mathbf{S}^{(3)} = \{A^{(3)}, B^{(3)}, C^{(3)}, D^{(3)}, E^{(3)}\}$, respectively. From the state $\{100, 100\}$, the network enters the state $\{010, 100\}$ with probability 1, and from the latter, two situations may occur: 1) If node S can hear R_2 (this happens with probability h_{02}), the network will enter the state $\{001, 100\}$, during which a packet will be transmitted with success to D (i.e., no interferences are present) and from which the network will come back to the initial state $\{100, 100\}$; 2) otherwise, the network will enter the state $\{101, 100\}$, where possible collisions may occur. From the latter state, if the packet sent by S is captured by R_1 (this happens with probability c_{02}), the network comes back to $\{010, 100\}$; otherwise, the network moves to state $\{000, 100\}$, where no transmissions occur, since according to the protocol, after a transmission S has to wait for W slots before transmitting the following packet because $W = 1$ at the subsequent slot the network will come back to the initial state, with probability 1.

The state probabilities vector is $\boldsymbol{\pi}^{(3)} = [\pi_{A^{(3)}}, \pi_{B^{(3)}}, \pi_{C^{(3)}}, \pi_{D^{(3)}}, \pi_{E^{(3)}}]^T$, where $[\cdot]^T$ denotes the transpose. The matrix of the state transition probabilities is given by

$$\mathbf{P}^{(3)} = \begin{bmatrix} 0 & 0 & 1 & 1 & 0 \\ 1 & 0 & 0 & 0 & c_{02} \\ 0 & h_{02} & 0 & 0 & 0 \\ 0 & 0 & 0 & 0 & \bar{c}_{02} \\ 0 & \bar{h}_{02} & 0 & 0 & 0 \end{bmatrix}.$$

To find the state probabilities, the following system should be solved:

$$\begin{cases} \pi_{A^{(3)}} + \pi_{B^{(3)}} + \pi_{C^{(3)}} + \pi_{D^{(3)}} + \pi_{E^{(3)}} = 1 \\ \boldsymbol{\pi}^{(3)} = \mathbf{P}^{(3)} \cdot \boldsymbol{\pi}^{(3)}. \end{cases} \quad (4)$$

By solving (4), we derive

$$\begin{aligned} \pi_{A^{(3)}} &= 1/3 h_{02} + 1/4 \bar{h}_{02} \bar{c}_{02} \\ \pi_{B^{(3)}} &= 1/3 h_{02} + 1/2 \bar{h}_{02} c_{02} + 1/4 \bar{h}_{02} \bar{c}_{02} \\ \pi_{C^{(3)}} &= 1/3 h_{02} \\ \pi_{D^{(3)}} &= 1/4 \bar{h}_{02} \bar{c}_{02} \\ \pi_{E^{(3)}} &= 1/4 \bar{h}_{02} \bar{c}_{02} + 1/2 \cdot \bar{h}_{02} c_{02}. \end{aligned}$$

At this point, $\hat{\Sigma}$ can be expressed as

$$\hat{\Sigma} = \hat{\Sigma}|_{h_{02}=1} \cdot h_{02} + \hat{\Sigma}|_{\bar{h}_{02} \bar{c}_{02}=1} \cdot \bar{h}_{02} \bar{c}_{02} c_{20} + \hat{\Sigma}|_{\bar{h}_{02} c_{02}=1} \cdot \bar{h}_{02} c_{02} c_{20} \quad (5)$$

where $\hat{\Sigma}|_{h_{02}=1} = \sum_{\forall i,j,\mathbf{q}^{(3)}} \pi_{ij1,\mathbf{q}^{(3)}}|_{h_{02}=1} = 1/3$, $\hat{\Sigma}|_{\bar{h}_{02} \bar{c}_{02}=1} = \sum_{\forall i,j,\mathbf{q}^{(3)}} \pi_{ij1,\mathbf{q}^{(3)}}|_{\bar{h}_{02} \bar{c}_{02}=1} = 1/4$, and $\hat{\Sigma}|_{\bar{h}_{02} c_{02}=1} = \sum_{\forall i,j,\mathbf{q}^{(3)}} \pi_{ij1,\mathbf{q}^{(3)}}|_{\bar{h}_{02} c_{02}=1} = 1/2$. Note that in (5), the second and third terms of the sum include c_{20} , which is the probability that the packet generated by R_2 is captured by D, when affected by the interference generated by the source. Such probability is included to account for possible losses of packets when affected by the interference generated by nodes that are behind in the chain (S in this case). As a result, we obtain

$$\hat{\Sigma} = 1/3 \cdot h_{02} + (1/4 \cdot \bar{h}_{02} \bar{c}_{02} + 1/2 \cdot \bar{h}_{02} c_{02}) c_{20}.$$

The success probability for the source, in the case of LWN, can be expressed as

$$p_S = p_S|_{h_{02}=1} \cdot h_{02} + p_S|_{\bar{h}_{02} \bar{c}_{02}=1} \cdot \bar{h}_{02} \bar{c}_{02} c_{20} + p_S|_{\bar{h}_{02} c_{02}=1} \cdot \bar{h}_{02} c_{02} c_{20}$$

where

$$\begin{aligned} p_S|_{h_{02}=1} &= \frac{\sum_{\forall i,j,\mathbf{q}^{(3)}} \pi_{ij1,\mathbf{q}^{(3)}}}{\sum_{\forall j,k,\mathbf{q}^{(3)}} \pi_{1jk,\mathbf{q}^{(3)}}|_{h_{02}=1}} = 1 \\ p_S|_{\bar{h}_{02} \bar{c}_{02}=1} &= \frac{\sum_{\forall i,j,\mathbf{q}^{(3)}} \pi_{ij1,\mathbf{q}^{(3)}}}{\sum_{\forall j,k,\mathbf{q}^{(3)}} \pi_{1jk,\mathbf{q}^{(3)}}|_{\bar{h}_{02} \bar{c}_{02}=1}} = \frac{1}{2} \\ p_S|_{\bar{h}_{02} c_{02}=1} &= \frac{\sum_{\forall i,j,\mathbf{q}^{(3)}} \pi_{ij1,\mathbf{q}^{(3)}}}{\sum_{\forall j,k,\mathbf{q}^{(3)}} \pi_{1jk,\mathbf{q}^{(3)}}|_{\bar{h}_{02} c_{02}=1}} = 1. \end{aligned}$$

Therefore

$$p_S = h_{02} + (1/2 \cdot \bar{h}_{02} \bar{c}_{02} + \bar{h}_{02} c_{02}) c_{20}.$$

Finally, with reference to the LWSN case, the average success probability can be expressed as

$$\bar{p}_S = \bar{p}_S|_{h_{02}=1} \cdot h_{02} + \bar{p}_S|_{\bar{h}_{02} \bar{c}_{02}=1} \cdot \bar{h}_{02} \bar{c}_{02} c_{20} + \bar{p}_S|_{\bar{h}_{02} c_{02}=1} \cdot \bar{h}_{02} c_{02} c_{20}$$

where

$$\begin{aligned} \bar{p}_S|_{h_{02}=1} &= \frac{\sum_{\forall i,j,\mathbf{q}^{(3)}} \pi_{ij1,\mathbf{q}^{(3)}}}{\sum_{\forall i,j,k,\mathbf{q}^{(3)}} (i+j+k) \pi_{ijk,\mathbf{q}^{(3)}}|_{h_{02}=1}} = 1 \\ \bar{p}_S|_{\bar{h}_{02} \bar{c}_{02}=1} &= \frac{\sum_{\forall i,j,\mathbf{q}^{(3)}} \pi_{ij1,\mathbf{q}^{(3)}}}{\sum_{\forall i,j,k,\mathbf{q}^{(3)}} (i+j+k) \pi_{ijk,\mathbf{q}^{(3)}}|_{\bar{h}_{02} \bar{c}_{02}=1}} = \frac{3}{4} \\ \bar{p}_S|_{\bar{h}_{02} c_{02}=1} &= \frac{\sum_{\forall i,j,\mathbf{q}^{(3)}} \pi_{ij1,\mathbf{q}^{(3)}}}{\sum_{\forall i,j,k,\mathbf{q}^{(3)}} (i+j+k) \pi_{ijk,\mathbf{q}^{(3)}}|_{\bar{h}_{02} c_{02}=1}} = 1 \end{aligned}$$

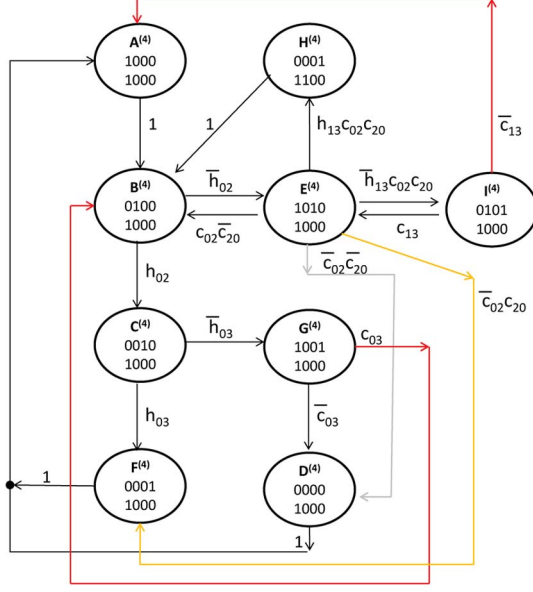


Fig. 4. Finite-state transition diagram for a four-hop network.

resulting in

$$\bar{p}_S = h_{02} + (3/4 \cdot \bar{h}_{02} \bar{c}_{02} + \bar{h}_{02} c_{02}) c_{20}.$$

D. Four-Hop Network

The finite-state transition diagram is reported in Fig. 4. The set of states in this case is: $\mathbf{S}^{(4)} = \{\{1000, 1000\}, \{0100, 1000\}, \{0010, 1000\}, \{0000, 1000\}, \{1010, 1000\}, \{0001, 1000\}, \{1001, 1000\}, \{0001, 1100\}, \{0101, 1000\}\} = \{A^{(4)}, B^{(4)}, C^{(4)}, D^{(4)}, E^{(4)}, F^{(4)}, G^{(4)}, H^{(4)}, I^{(4)}\}$. The state probabilities vector is $\boldsymbol{\pi}^{(4)} = [\pi_{A^{(4)}}, \pi_{B^{(4)}}, \pi_{C^{(4)}}, \pi_{D^{(4)}}, \pi_{E^{(4)}}, \pi_{F^{(4)}}, \pi_{G^{(4)}}, \pi_{H^{(4)}}, \pi_{I^{(4)}}]^T$, and $\mathbf{P}^{(4)}$ is given by

$$\mathbf{P}^{(4)} = \begin{bmatrix} 0 & 0 & 0 & 1 & 0 & 1 & 0 & 0 & \bar{c}_{13} \\ 1 & 0 & 0 & 0 & c_{02} \bar{c}_{20} & 0 & c_{03} & 1 & 0 \\ 0 & h_{02} & 0 & 0 & 0 & 0 & 0 & 0 & 0 \\ 0 & 0 & 0 & 0 & \bar{c}_{02} \bar{c}_{20} & 0 & \bar{c}_{03} & 0 & 0 \\ 0 & \bar{h}_{02} & 0 & 0 & 0 & 0 & 0 & 0 & c_{13} \\ 0 & 0 & h_{03} & 0 & \bar{c}_{02} c_{20} & 0 & 0 & 0 & 0 \\ 0 & 0 & \bar{h}_{03} & 0 & 0 & 0 & 0 & 0 & 0 \\ 0 & 0 & 0 & 0 & h_{13} c_{02} c_{20} & 0 & 0 & 0 & 0 \\ 0 & 0 & 0 & 0 & \bar{h}_{13} c_{02} c_{20} & 0 & 0 & 0 & 0 \end{bmatrix}.$$

To find the state probabilities, the following system should be solved:

$$\begin{cases} \pi_{A^{(4)}} + \pi_{B^{(4)}} + \pi_{C^{(4)}} + \pi_{D^{(4)}} + \pi_{E^{(4)}} + \pi_{F^{(4)}} \\ + \pi_{G^{(4)}} + \pi_{H^{(4)}} + \pi_{I^{(4)}} = 1 \\ \boldsymbol{\pi}^{(4)} = \mathbf{P}^{(4)} \cdot \boldsymbol{\pi}^{(4)}. \end{cases}$$

The states probabilities are given by

$$\begin{aligned} \pi_{A^{(4)}} &= 1/4 h_{02} h_{03} + 1/4 \bar{h}_{02} \bar{c}_{02} + 1/5 h_{02} \bar{h}_{03} \bar{c}_{03} \\ &\quad + 1/4 \bar{h}_{02} c_{02} c_{20} \bar{h}_{13} \bar{c}_{13} \\ \pi_{B^{(4)}} &= 1/5 h_{02} + 1/20 h_{02} h_{03} + 2/15 h_{02} \bar{h}_{03} c_{03} \\ &\quad + 1/2 \bar{h}_{02} c_{02} \bar{c}_{20} + 1/4 \bar{h}_{02} \bar{c}_{02} \\ &\quad + \bar{h}_{02} c_{02} c_{20} (1/3 h_{13} + 1/4 \bar{h}_{13} \bar{c}_{13}) \\ \pi_{C^{(4)}} &= 1/4 h_{02} h_{03} + h_{02} \bar{h}_{03} (1/3 c_{03} + 1/5 \bar{c}_{03}) \\ \pi_{D^{(4)}} &= 1/5 h_{02} \bar{h}_{03} \bar{c}_{03} + 1/4 \bar{h}_{02} \bar{c}_{02} \bar{c}_{20} \\ \pi_{E^{(4)}} &= 1/2 \bar{h}_{02} c_{02} \bar{c}_{20} + 1/4 \bar{h}_{02} \bar{c}_{02} + \bar{h}_{02} c_{02} c_{20} \\ &\quad \cdot (1/3 h_{13} + 1/4 \bar{h}_{13} (1 + c_{13})) \\ \pi_{F^{(4)}} &= 1/4 h_{02} h_{03} + 1/4 \bar{h}_{02} \bar{c}_{02} c_{20} \\ \pi_{G^{(4)}} &= 1/5 h_{02} \bar{h}_{03} (1 + 2/3 c_{03}) \\ \pi_{H^{(4)}} &= 1/3 \bar{h}_{02} h_{13} c_{02} c_{20} \\ \pi_{I^{(4)}} &= 1/4 \bar{h}_{02} \bar{h}_{13} c_{02} c_{20} (1 + c_{13}). \end{aligned}$$

Then, applying the same procedure defined for the three-hop case, we get the performance metrics reported in (6), shown at the bottom of the page.

E. Five-Hop Network

The five-hop-case model is presented here. Due to the complexity of the model, a simplified analysis for this case has also been developed, still bringing very good results. This analysis is reported in the technical report of this paper [40].

In Fig. 5, we show the finite-state transition diagram describing the behavior of the network, with the indication about the different states $\mathbf{S}^{(5)} = \{A^{(5)}, \dots, V^{(5)}\}$. The matrix of the state transition probabilities $\mathbf{P}^{(5)}$ is given by (7), shown at the bottom of the page.

By solving the equation system similar to (4), we can derive the state probabilities vector, i.e., $\boldsymbol{\pi}^{(5)}$. For the sake of conciseness, we report in (8), shown at the bottom of the page, a single formula that is valid to derive all the states probabilities (which is denoted generically as π) by changing the parameters included in the formula. The value of the parameters α_k for $k = 1, \dots, 35$ to be set are reported in Table I, where the apex $^{(5)}$ is omitted for the sake of space.

For the sake of conciseness, we report a single formula that is valid to derive all the three performance metrics (denote generically as M), $\hat{\Sigma}$, p_S , and \bar{p}_S , by changing the parameters included in the formula. In particular, by applying the same procedure defined for the other scenarios, we get (9), shown at the bottom of the page, for M , where the values of the parameters β_k for $k = 1, \dots, 35$ to be set are reported in Table II.

$$\begin{aligned} \hat{\Sigma} &= 1/4 h_{02} h_{03} + h_{02} \bar{h}_{03} (1/3 c_{03} c_{30} + 1/5 \bar{c}_{03} c_{30}) + 1/4 \bar{h}_{02} \bar{c}_{02} c_{20} + 1/3 \bar{h}_{02} h_{13} c_{02} c_{20} + 1/2 \bar{h}_{02} \bar{h}_{13} c_{02} c_{20} \cdot (c_{13} c_{31} + 1/2 \bar{c}_{13} c_{31}) \\ p_S &= h_{02} h_{03} + h_{02} \bar{h}_{03} (c_{03} c_{30} + 1/2 \bar{c}_{03} c_{30}) + 1/2 \bar{h}_{02} \bar{c}_{02} c_{20} + \bar{h}_{02} h_{13} c_{02} c_{20} + \bar{h}_{02} \bar{h}_{13} c_{02} c_{20} (c_{13} c_{31} + 1/2 \bar{c}_{13} c_{31}) \\ \bar{p}_S &= h_{02} h_{03} + h_{02} \bar{h}_{03} (c_{03} c_{30} + 4/5 \bar{c}_{03} c_{30}) + 4/5 \bar{h}_{02} \bar{c}_{02} c_{20} + \bar{h}_{02} h_{13} c_{02} c_{20} + \bar{h}_{02} \bar{h}_{13} c_{02} c_{20} (c_{13} c_{31} + 2/3 \bar{c}_{13} c_{31}) \end{aligned} \quad (6)$$

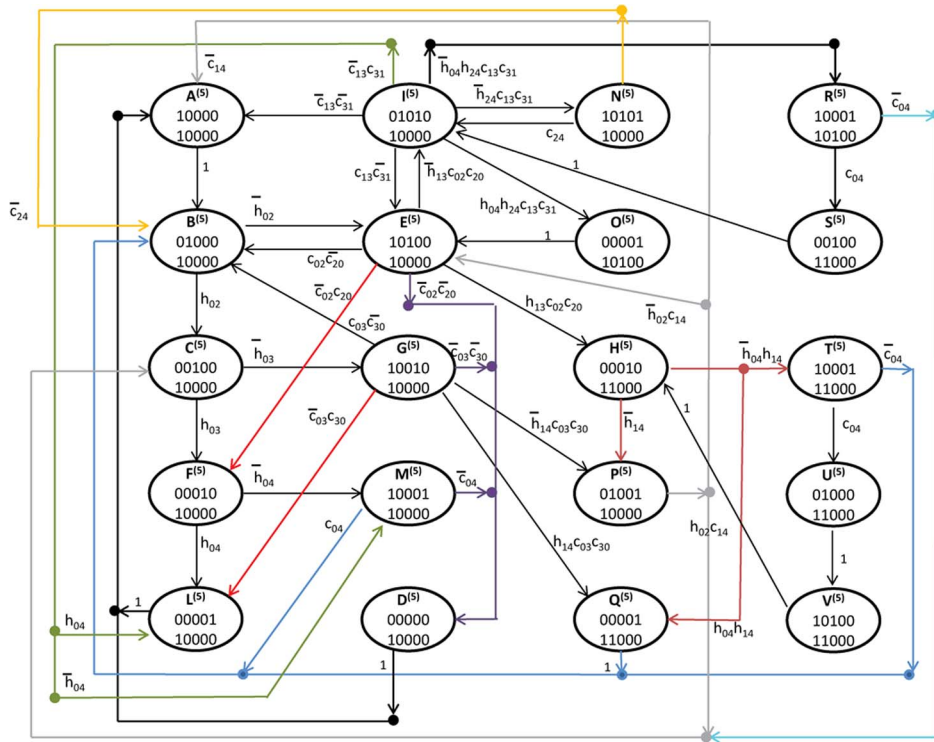


Fig. 5. Finite-state transition diagram for a five-hop network.

VI. BENCHMARK PROTOCOLS

In the following section, the performance of L-CSMA is compared with that obtained when using three different slotted and contention-based protocols suitable for WSNs: 1) IEEE 802.15.4 (in beacon-enabled mode), which is the de facto standard for WSNs; 2) Ripple, which is a token-based protocol [36]; and 3) slotted ALOHA.

IEEE 802.15.4 works in the 2.4-GHz band, using a bit rate of 250 kbit/s. We refer to the standard for a complete description of the IEEE 802.15.4 MAC protocol [37], but here, we recall that in beacon-enabled mode, time is divided into slots of $320 \mu\text{s}$ each and that each node has to sense the channel for two subsequent slots (of $320 \mu\text{s}$ each) before transmitting the packet, bringing a sensing duration at each attempt of $640 \mu\text{s}$. Each time a node finds the channel busy, a random delay (backoff)

[illegible]

$$\begin{aligned}
\pi = & h_{02} \{ h_{03} [\alpha_1 \cdot h_{04} + \bar{h}_{04}(\alpha_2 \cdot c_{04} + \alpha_3 \cdot \bar{c}_{04})] + \bar{h}_{03} [c_{03}c_{30} (\alpha_4 \cdot h_{14} + \bar{h}_{14}(\alpha_5 \cdot c_{14} + \alpha_6 \cdot \bar{c}_{14})) + \alpha_7 \cdot \bar{c}_{03}c_{30} \\
& + \alpha_8 \cdot c_{03}\bar{c}_{30} + \alpha_9 \cdot \bar{c}_{03}\bar{c}_{30}] \} + \bar{h}_{02}c_{02}c_{20} \{ h_{13} [h_{14} (\alpha_{10} \cdot h_{04} + \bar{h}_{04}(\alpha_{11} \cdot c_{04} + \alpha_{12} \cdot \bar{c}_{04})) + \bar{h}_{14}(\alpha_{13} \cdot c_{14} + \alpha_{14} \cdot \bar{c}_{14})] \\
& + \bar{h}_{13} [c_{13}c_{31} (\bar{h}_{24}(\alpha_{15} \cdot c_{24} + \alpha_{16} \cdot \bar{c}_{24}) + h_{24}\bar{h}_{04} (\alpha_{17} \cdot c_{04} + \alpha_{18} \cdot h_{03}\bar{c}_{04} + \bar{h}_{03} (\bar{c}_{04}(\alpha_{19} \cdot c_{03}\bar{c}_{30} + \alpha_{20} \cdot \bar{c}_{03}\bar{c}_{30}) \\
& + \bar{h}_{14}c_{03}c_{30}(\alpha_{21} \cdot c_{14}\bar{c}_{04} + \alpha_{22} \cdot \bar{c}_{14}\bar{c}_{04}) + c_{30}\bar{c}_{04}(\alpha_{23} \cdot h_{14}c_{03} + \alpha_{24} \cdot \bar{c}_{03})))] + \bar{c}_{13}c_{31} (\alpha_{25} \cdot h_{04} + \bar{h}_{04}(\alpha_{26} \cdot c_{04} + \alpha_{27} \cdot \bar{c}_{04})) \\
& + \alpha_{28} \cdot h_{04}h_{24}c_{13}c_{31} + \alpha_{29} \cdot c_{13}\bar{c}_{31} + \alpha_{30} \cdot \bar{c}_{13}\bar{c}_{31}] \} + \bar{h}_{02}\bar{c}_{02}c_{20} [\alpha_{31} \cdot h_{04} + \bar{h}_{04}(\alpha_{32} \cdot c_{04} + \alpha_{33} \cdot \bar{c}_{04})] \\
& + \bar{h}_{02} (\alpha_{34} \cdot c_{02}\bar{c}_{20} + \alpha_{35} \cdot \bar{c}_{02}\bar{c}_{20}) \} \tag{8}
\end{aligned}$$

$$\begin{aligned}
M = & h_{02} \{ h_{03} [\beta_1 \cdot h_{04} + \bar{h}_{04}c_{40}(\beta_2 \cdot c_{04} + \beta_3 \cdot \bar{c}_{04})] + \bar{h}_{03} [c_{03}c_{30} (\beta_4 \cdot h_{14} + \bar{h}_{14}c_{41}(\beta_5 \cdot c_{14} + \beta_6 \cdot \bar{c}_{14})) + \beta_7 \cdot \bar{c}_{03}c_{30}] \} \\
& + \bar{h}_{02}c_{02}c_{20} \{ h_{13} [h_{14} (\beta_8 \cdot h_{04} + \bar{h}_{04}c_{40}(\beta_9 \cdot c_{04} + \beta_{10} \cdot \bar{c}_{04})) + \bar{h}_{14}c_{41}(\beta_{11} \cdot c_{14} + \beta_{12} \cdot \bar{c}_{14})] \\
& + \bar{h}_{13} [c_{13}c_{31} (\bar{h}_{24}c_{42}(\beta_{13} \cdot c_{24} + \beta_{14} \cdot \bar{c}_{24}) + h_{24}\bar{h}_{04} (\beta_{15} \cdot c_{04}c_{40} + \beta_{16} \cdot h_{03}\bar{c}_{04}c_{40} + \bar{h}_{03} (\bar{c}_{04}c_{40}(\beta_{17} \cdot c_{03}\bar{c}_{30} + \beta_{18} \cdot \bar{c}_{03}\bar{c}_{30}) \\
& + \bar{h}_{14}c_{03}c_{30} (c_{14}\bar{c}_{04}(\beta_{19} \cdot c_{40}c_{41} + \beta_{20} \cdot \bar{c}_{40}c_{41} + \beta_{21} \cdot c_{40}\bar{c}_{41}) + \bar{c}_{14}\bar{c}_{04}(\beta_{22} \cdot c_{40}c_{41} + \beta_{23} \cdot \bar{c}_{40}c_{41} + \beta_{24} \cdot c_{40}\bar{c}_{41})) \\
& + h_{14}c_{03}c_{30}\bar{c}_{04}(\beta_{25} \cdot c_{40} + \beta_{26} \cdot \bar{c}_{40}) + \bar{c}_{03}c_{30}\bar{c}_{04}(\beta_{27} \cdot c_{40} + \beta_{28} \cdot \bar{c}_{40})))] + \bar{c}_{13}c_{31} (\beta_{29} \cdot h_{04} + \bar{h}_{04}c_{40}(\beta_{30} \cdot c_{04} + \beta_{31} \cdot \bar{c}_{04})) \\
& + \beta_{32} \cdot h_{04}h_{24}c_{13}c_{31}] \} + \bar{h}_{02}\bar{c}_{02}c_{20} [\beta_{33} \cdot h_{04} + \bar{h}_{04}c_{40}(\beta_{34} \cdot c_{04} + \beta_{35} \cdot \bar{c}_{04})] \} \tag{9}
\end{aligned}$$

is introduced before trying to access the channel again. The slot for this protocol has a different meaning with respect to the L-CSMA case, where it includes sensing and transmission time. For the latter reason, performance is compared in terms of success probability and throughput and not in terms of normalized throughput.

The Ripple protocol described in [36] is also considered. In particular, we enhanced the IEEE 802.15.4⁴ through the transmission of three control packets, i.e., RTS, CTS, and RTR, used to avoid the hidden-terminal problem and acting as tokens in the line. In particular, RTS is used as a token in the downstream (from the source to the destination), whereas RTR is used as a token in the upstream (from D to S).

In pure slotted ALOHA, when a node has a packet ready to be transmitted, it will transmit it at the beginning of the following slot. Such protocol has a low success probability when used in multihop networks; therefore, in this paper, we consider a smarter version of the protocol, where we impose that each node transmits the packet with a probability that is a function of the number of relays in the network and set equal to $1/(n+1)$. In this case, time is divided into slots of duration T_{slot} , where each slot just contains the data packet. The latter implies that in the case of LWNs, we have $T_{\text{slot}} = Z/R_b$, whereas in the case of LWSNs, we have $T_{\text{slot}} = (n+1) \cdot P/R_b + H/R_b$.

For the sake of fairness in the comparison, the same applications, i.e., LWN and LWSN, are considered by apply-

ing the same data aggregation strategy used for L-CSMA. Moreover, power control is used, and no retransmissions are allowed.

VII. NUMERICAL RESULTS

Here, we show numerical results achieved through the mathematical model described in Section V and through a simulator, written in C, implementing the two reference scenarios and the different protocols considered, as they have been described in the previous sections. In particular, the simulator implements the LWN and LWSN applications described in Sections III-B and C and the channel and packet capture models described in Section III-A. With reference to the latter, for each transmitted packet, the total level of interfering power (i.e., I as the sum of the interfering power) is computed, and the signal-to-interference ratio is compared with the threshold, i.e., α , to decide if the packet has been received or not. Therefore, the total level of interference is accounted for. This will allow determination of the level of accuracy of the model, which accounts only for the nearest interferer. The simulator has been validated in [40] through comparison with results achieved using an NS-3 simulator and experiments performed with TI CC 2530 devices. See [40] for details on this.

In all simulations, results are achieved by averaging among 1000 different scenarios and 1000 different transmissions from S to D per scenario. Each scenario is characterized by a different fading sample symmetric matrix (obtained by extracting independent samples of a negative exponential random variable with unit mean) and maintaining the same channel matrix for the

⁴Although the protocol has been originally proposed for IEEE 802.11, we apply it to 802.15.4 because it is our reference standard.

TABLE I
PARAMETER SETTING FOR THE FIVE-HOP SCENARIO

	π_A	π_B	π_C	π_D	π_E	π_F	π_G	π_H	π_I	π_L	π_M	π_N	π_O	π_P	π_Q	π_R	π_S	π_T	π_U	π_V
α_1	1/5	1/5	1/5	0	0	1/5	0	0	0	1/5	0	0	0	0	0	0	0	0	0	0
α_2	0	1/4	1/4	0	0	1/4	0	0	0	0	1/4	0	0	0	0	0	0	0	0	0
α_3	1/6	1/6	1/6	1/6	0	1/6	0	0	0	0	1/6	0	0	0	0	0	0	0	0	0
α_4	0	1/4	1/4	0	0	0	1/4	0	0	0	0	0	0	0	1/4	0	0	0	0	0
α_5	0	0	1/3	0	0	0	1/3	0	0	0	0	0	0	1/3	0	0	0	0	0	0
α_6	1/5	1/5	1/5	0	0	0	1/5	0	0	0	0	0	0	1/5	0	0	0	0	0	0
α_7	1/5	1/5	1/5	0	0	0	1/5	0	0	1/5	0	0	0	0	0	0	0	0	0	0
α_8	0	1/3	1/3	0	0	0	1/3	0	0	0	0	0	0	0	0	0	0	0	0	0
α_9	1/5	1/5	1/5	1/5	0	0	1/5	0	0	0	0	0	0	0	0	0	0	0	0	0
α_{10}	0	1/4	0	0	1/4	0	0	1/4	0	0	0	0	0	0	1/4	0	0	0	0	0
α_{11}	0	0	0	0	0	0	0	1/4	0	0	0	0	0	0	0	0	1/4	1/4	1/4	0
α_{12}	0	1/4	0	0	1/4	0	0	1/4	0	0	0	0	0	0	0	0	1/4	0	0	0
α_{13}	0	0	0	0	1/3	0	0	1/3	0	0	0	0	0	1/3	0	0	0	0	0	0
α_{14}	1/5	1/5	0	0	1/5	0	0	1/5	0	0	0	0	0	1/5	0	0	0	0	0	0
α_{15}	0	0	0	0	0	0	0	0	1/2	0	0	1/2	0	0	0	0	0	0	0	0
α_{16}	0	1/4	0	0	1/4	0	0	0	1/4	0	0	1/4	0	0	0	0	0	0	0	0
α_{17}	0	0	0	0	0	0	0	0	1/3	0	0	0	0	0	0	1/3	0	0	0	1/3
α_{18}	1/9	1/9	1/9	1/9	1/9	1/9	0	0	1/9	0	1/9	0	0	0	0	1/9	0	0	0	0
α_{19}	0	1/6	1/6	0	1/6	0	1/6	0	1/6	0	0	0	0	0	0	1/6	0	0	0	0
α_{20}	1/8	1/8	1/8	1/8	1/8	0	1/8	0	1/8	0	0	0	0	0	0	1/8	0	0	0	0
α_{21}	0	0	1/6	0	1/6	0	1/6	0	1/6	0	0	0	0	1/6	0	1/6	0	0	0	0
α_{22}	1/8	1/8	1/8	0	1/8	0	1/8	0	1/8	0	0	0	0	1/8	0	1/8	0	0	0	0
α_{23}	0	1/7	1/7	0	1/7	0	1/7	0	1/7	0	0	0	0	0	1/7	1/7	0	0	0	0
α_{24}	1/8	1/8	1/8	0	1/8	0	1/8	0	1/8	1/8	0	0	0	0	0	1/8	0	0	0	0
α_{25}	1/5	1/5	0	0	1/5	0	0	0	1/5	1/5	0	0	0	0	0	0	0	0	0	0
α_{26}	0	1/4	0	0	1/4	0	0	0	1/4	0	1/4	0	0	0	0	0	0	0	0	0
α_{27}	1/6	1/6	0	1/6	1/6	0	0	0	1/6	0	1/6	0	0	0	0	0	0	0	0	0
α_{28}	0	0	0	0	1/3	0	0	0	1/3	0	0	0	1/3	0	0	0	0	0	0	0
α_{29}	0	0	0	0	1/2	0	0	0	1/2	0	0	0	0	0	0	0	0	0	0	0
α_{30}	1/4	1/4	0	0	1/4	0	0	0	1/4	0	0	0	0	0	0	0	0	0	0	0
α_{31}	1/5	1/5	0	0	1/5	1/5	0	0	0	1/5	0	0	0	0	0	0	0	0	0	0
α_{32}	0	1/4	0	0	1/4	1/4	0	0	0	0	1/4	0	0	0	0	0	0	0	0	0
α_{33}	1/6	1/6	0	1/6	1/6	1/6	0	0	0	0	1/6	0	0	0	0	0	0	0	0	0
α_{34}	0	1/2	0	0	1/2	0	0	0	0	0	0	0	0	0	0	0	0	0	0	0
α_{35}	1/4	1/4	0	1/4	1/4	0	0	0	0	0	0	0	0	0	0	0	0	0	0	0

TABLE II
PARAMETER SETTING FOR THE FIVE-HOP SCENARIO

	$\hat{\Sigma}$	p_S	\bar{p}_S		$\hat{\Sigma}$	p_S	\bar{p}_S		$\hat{\Sigma}$	p_S	\bar{p}_S
β_1	1/5	1	1	β_{13}	1/2	1	1	β_{25}	2/7	2/3	10/11
β_2	1/4	1	1	β_{14}	1/4	1/2	5/8	β_{26}	1/7	1/3	5/11
β_3	1/6	1/2	5/6	β_{15}	1/3	1	1	β_{27}	1/4	1/2	5/6
β_4	1/4	1	1	β_{16}	2/9	1/2	5/6	β_{28}	1/8	1/4	5/12
β_5	1/3	1	1	β_{17}	1/6	1/3	1/2	β_{29}	1/5	1/2	5/7
β_6	1/5	1/2	5/7	β_{18}	1/8	1/4	5/11	β_{30}	1/4	1/2	5/7
β_7	1/5	1/2	5/6	β_{19}	1/3	2/3	10/11	β_{31}	1/6	1/3	5/8
β_8	1/4	1	1	β_{20}	1/6	1/3	5/11	β_{32}	1/3	1	1
β_9	1/4	1/2	5/6	β_{21}	1/6	1/3	5/11	β_{33}	1/5	1/2	5/6
β_{10}	1/4	1/2	5/6	β_{22}	1/4	1/2	10/13	β_{34}	1/4	1/2	5/6
β_{11}	1/3	1	1	β_{23}	1/8	1/4	5/13	β_{35}	1/6	1/3	5/7
β_{12}	1/5	1/2	5/7	β_{24}	1/8	1/4	5/13				

burst of 1000 transmissions, so that proper possible correlations among links are accounted for.

The simulator parameters, when no otherwise specified, are set as follows: $R_b = 250$ kbit/s, $k = -40$ dB (considering a frequency of 2.4 GHz as that used by 802.15.4), $H = 160$ bits (20 bytes), $P = 160$ bits (20 bytes), $d = 40$ m, $\beta = 3$, $\alpha = 5$ dB, $P_{R_{\min}} = -90$ dBm, and $W = 1$. We also set the size of RTS, CTS, and RTR packets equal to 20 bytes. For fair comparison among the different protocols, we set the same bit rate for all cases, and we set the minimum sensing duration, i.e., T , for L-CSMA equal to $640 \mu s$, corresponding to the sensing duration for the 802.15.4 and Ripple cases that are also equal to the transmission time of the considered payload (20 bytes), as

requested in L-CSMA. Finally, for the case of 802.15.4, MAC parameters are set to the default values [37]. If not otherwise specified, retransmissions are not allowed.

A. Validation of the Mathematical Model

Here, we compare the mathematical model results with simulation results. The scope of validation through simulation is to demonstrate that the simplifying assumptions described in Section V slightly affect performance.

In Fig. 6, we show the packet success probability, i.e., p_S , for the source in the case of LWN, as a function of the sensing threshold, i.e., $P_{S_{\min}}$, when considering the model

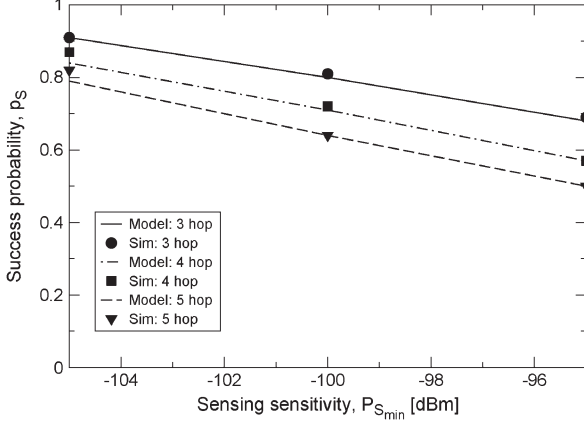


Fig. 6. p_S as a function of $P_{S_{min}}$: Simulations and model results.

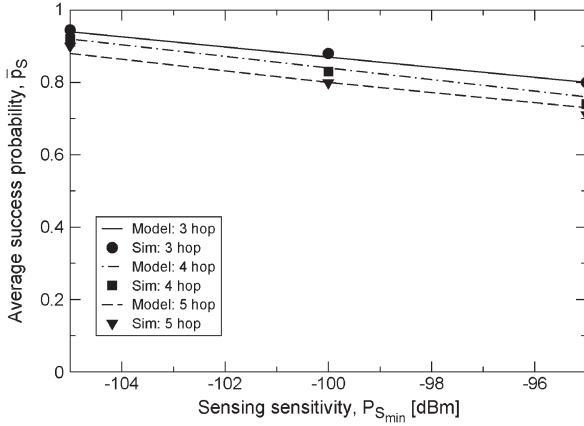


Fig. 7. \bar{p}_S as a function of $P_{S_{min}}$: Simulations and model results.

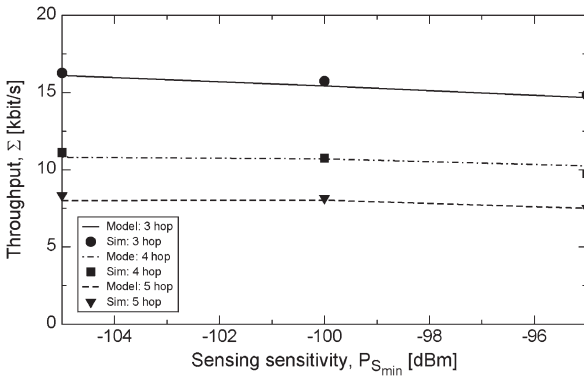


Fig. 8. Σ as a function of $P_{S_{min}}$: Simulations and model results.

and simulations, for the cases of three, four, and five hops, respectively. In this case, we set $P = 800$ bits (100 bytes). As can be seen, slight differences are present in the case of five hops, due to the impact of not considering the correlation among the capturing probabilities. Fig. 7 refers to the LWSN case, i.e., we show the average success probability \bar{p}_S , when varying $P_{S_{min}}$ and setting $P = 160$ bits (20 bytes). Finally, Fig. 8 shows the source throughput Σ as a function of $P_{S_{min}}$ considering the LWSN case and $P = 160$ bits (20 bytes). In all cases, simulations and mathematical model results are compared: A perfect agreement is found. With reference to the general behavior of the curves, we can note that the

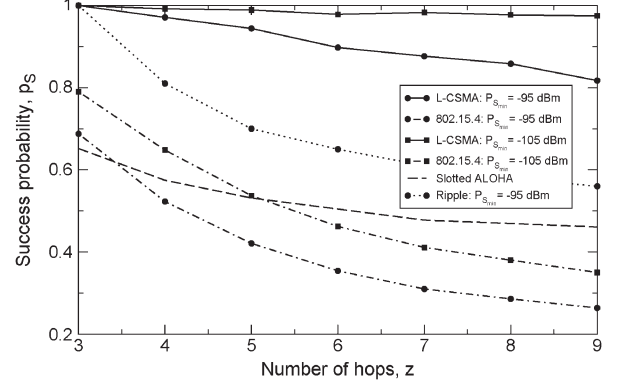


Fig. 9. p_S as a function of z for the LWN case.

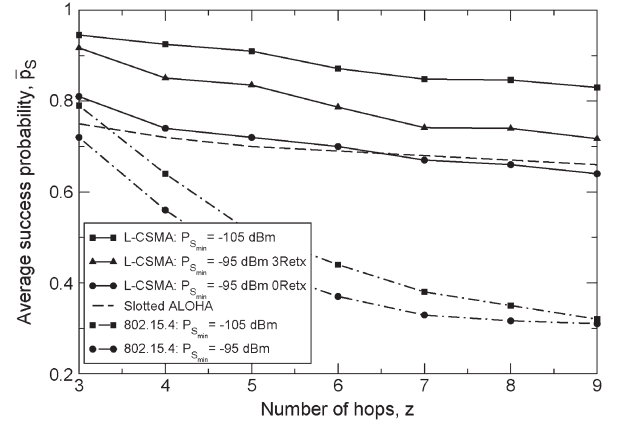


Fig. 10. \bar{p}_S as a function of z for the LWSN case.

success probability (averaged or not) decreases by increasing $P_{S_{min}}$ since the sensing capability of nodes worsens and more collisions are present. As a consequence, the throughput Σ slightly decreases with $P_{S_{min}}$ for the set of values considered in this figure (see below).

As for the dependence on the number of hops, all the metrics decrease by getting z larger, since more relays will compete for the channel and the collision probability increases.

B. L-CSMA Performance

Here, we compare the performance achievable through the L-CSMA protocol with those of IEEE 802.15.4, slotted ALOHA, and Ripple.

We first evaluate the performance in terms of p_S for the case of LWN as a function of the number of hops (see Fig. 9), for different values of $P_{S_{min}}$ (note that in the case of slotted ALOHA, the sensing threshold does not affect performance). In all cases, L-CSMA significantly outperforms the other protocols. As expected, Ripple outperforms 802.15.4 but still behaves worse than L-CSMA. Note that since in our protocol packets are lost only due to the presence of hidden node(s) causing a damaging collision, comparing the success probability coincides with comparing the probability of not having the hidden-terminal problem: Fig. 9 shows the improvement obtained in this regard with respect to 802.15.4.

The comparison related to the average success probability, i.e., \bar{p}_S , is shown in Fig. 10, considering the LWSN case.

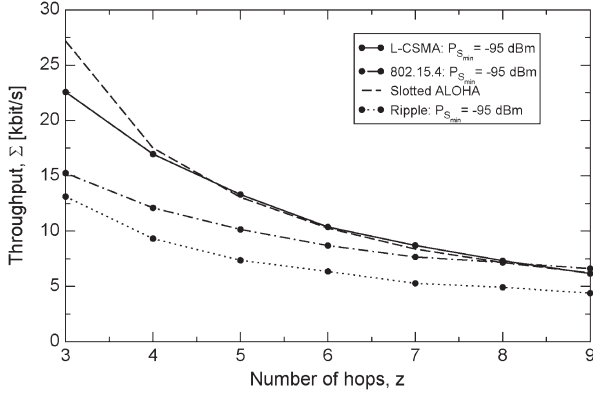


Fig. 11. Σ as a function of z for the LWN case.

Again, L-CSMA is the best solution, even if a proper setting of the sensing threshold is needed to obtain an improvement with respect to slotted ALOHA. Results related to Ripple are not included in this figure for the sake of readability, but they are included in the technical report [40]. As can be seen in [40, Fig. 3], Ripple has the worst performance with respect to L-CSMA, except for the case of three-hop networks, where performance is similar.

To demonstrate the applicability of L-CSMA to scenarios having a very strict requirement in terms of success probability, we evaluated the performance when retransmissions are applied. By assuming a perfect acknowledge mechanism (e.g., transmitting an explicit acknowledgement at the end of the slot using power control), we impose on each node to retransmit the packet up to a maximum number of times. The achieved improvement in terms of average success probability is shown in Fig. 10 for the case of three retransmissions (at maximum). However, results related to the throughput do not change. The latter is due to the fact that if a node retransmits a packet, the probability that it reaches the destination is larger; however, on the other hand, the node is occupying the resource for the retransmission, while inhibiting transmissions of new packets backward in the chain. The latter two effects are balanced, resulting in the same performance in terms of throughput with and without retransmissions.

We then show the source throughput, i.e., Σ , as a function of the number of hops, i.e., z , for the cases of LWN and LWSN in Figs. 11 and 12, respectively. Only the case of $P_{S_{\min}} = -95$ dBm is reported for the sake of readability of the plots; however, similar trends can be noted for the case of $P_{S_{\min}} = -105$ dBm. As can be seen, for the LWN case, slotted ALOHA is approximately performing as L-CSMA, since in slotted ALOHA, there is no time wasted for sensing. L-CSMA outperforms Ripple in all cases, since the transmission of RTS/CTS and RTR control packets in the latter reduces the throughput. Finally, with reference to 802.15.4, L-CSMA always performs better, apart from the case of nine hops and LWN, since in L-CSMA, by increasing z , it increases the guard time at each hop, resulting in a decreasing of the throughput. The latter is not true for the case of LWSN where no guard times are present and where the time resource in the L-CSMA is better used.

The improvement in terms of throughput with respect to 802.15.4 is obtained due to the reduction of the exposed-

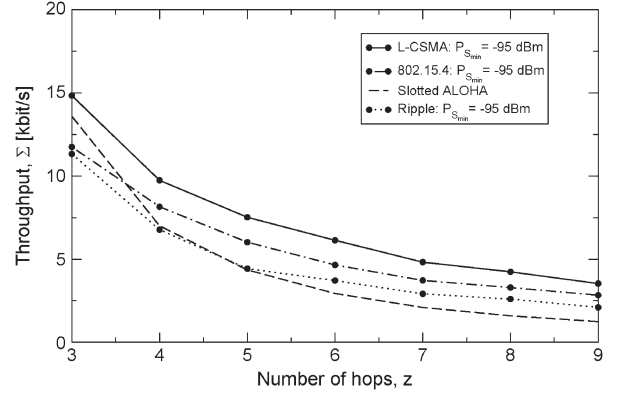


Fig. 12. Σ as a function of z for the LWSN case.

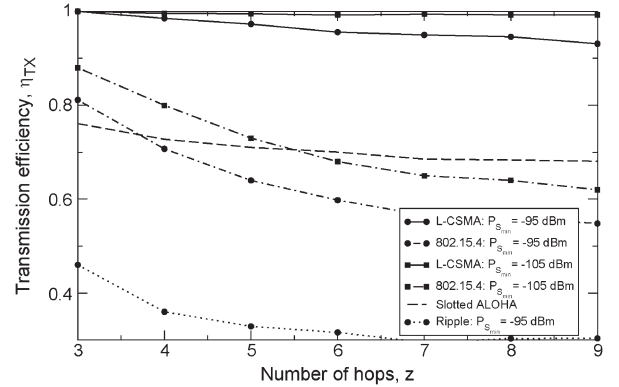


Fig. 13. η_{TX} as a function of z for the LWN case.

terminal problem. To demonstrate the latter, we evaluated the probability that a node finds the channel busy, that is, it is inhibited while its transmission would have not caused any packet loss. The latter probability is shown in Table III for L-CSMA and 802.15.4 and for the different nodes in the network, source, and relays. Results have been achieved by considering the LWSN case and by setting $P_{S_{\min}} = -95$ dBm. The comparison shows the notable improvement achieved with L-CSMA, since nodes are inhibited only by those forward in the line, resulting in no inhibition of nodes at the end of the line.

To demonstrate the efficiency of the protocol in the use of resources, resulting also in an efficient use of energy, we define the transmission efficiency, i.e., η_{TX} , as the ratio between the time spent for transmitting successful packets (i.e., without collisions) and the total time spent in transmission (for the transmission of both successfully transmitted packets and unsuccessfully transmitted packets). Results are reported in Figs. 13 and 14 for the LWN and LWSN cases, respectively. As can be seen, in all cases, the proposed protocol outperforms the existing protocols.

We conclude by showing (using the mathematical model) in Fig. 15 that there exists an optimum value of $P_{S_{\min}}$ maximizing the throughput for the cases of four and five hops. The latter is due to the fact that for low values of $P_{S_{\min}}$, throughput increases with the sensing sensitivity, since the exposed-terminal problem is reduced, and nodes are less inhibited. For higher values of $P_{S_{\min}}$, an increase of $P_{S_{\min}}$ worsens the hidden-terminal problem, causing losses and throughput decrease. Therefore,

TABLE III
PROBABILITY OF HAVING AN EXPOSED-TERMINAL PROBLEM

Node	3hop: 802.15.4	3hop: L-CSMA	4hop: 802.15.4	4hop: L-CSMA	5hop: 802.15.4	5hop: L-CSMA
S	0.28	0.13	0.27	0.14	0.28	0.14
R ₁	0.13	0	0.14	0.01	0.13	0.02
R ₂	0.02	0	0.12	0	0.13	0
R ₃	N.A.	N.A.	0.028	0	0.11	0
R ₄	N.A.	N.A.	N.A.	N.A.	0.03	0

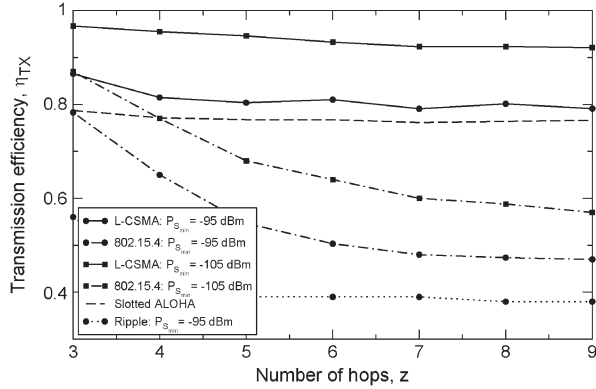


Fig. 14. η_{TX} as a function of z for the LWSN case.

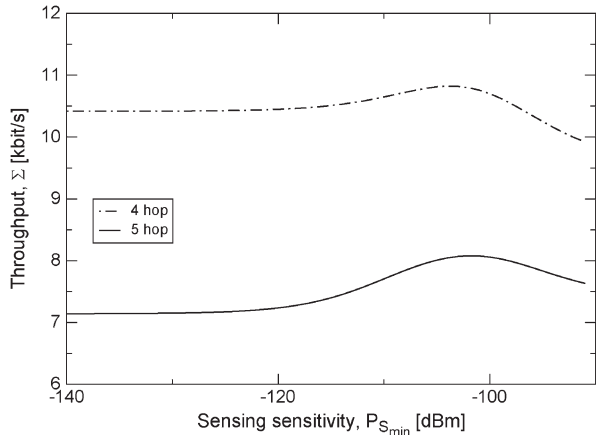


Fig. 15. Σ as a function of $P_{S_{min}}$ for four and five hops.

the optimum is reached when a good tradeoff between the reduction of the exposed-terminal problem and that of the hidden-terminal problem is reached. The model is a useful tool to quickly derive the optimum.

VIII. CONCLUSION

This paper has presented L-CSMA, which is a new MAC protocol for multihop LWNs, and a novel mathematical model for its assessment in interference-limited conditions. The protocol can be useful for LWNs, where only one source is generating data toward a given destination, but for LWSNs as well, where a set of nodes, deployed on a line, have a packet to be transmitted toward a single destination. Results show that the proposed protocol outperforms some of the existing protocols, such as IEEE 802.15.4 and Ripple, which is a token-based protocol recently presented in the literature. The proposed mathematical framework provides a good insight into the modeling of

multihop networks, because it introduces the idea of defining the generic state at the network level instead of the node level—an approach that has never been proposed in the literature before. In particular, the network status is modeled through a set of bits indicating the status (activity or not) of the corresponding hop. The model has been validated through comparison with simulations.

ACKNOWLEDGMENT

The authors would thank A. Stajkic for the useful discussions on the model.

REFERENCES

- [1] I. Jawhar and N. Mohamed, "A hierarchical and topological classification of linear sensor networks," in *Proc. WTS*, Apr. 2009, pp. 1–8.
- [2] Z. Wang, X. Zhao, and X. Qian, "The application and issues of linear wireless sensor networks," in *Proc. Int. Conf. ICSEM*, Oct. 2011, vol. 2, pp. 9–12.
- [3] I. Stoianov, L. Nachman, S. Madden, T. Tokmouline, and M. Csail, "PIPETNET: A wireless sensor network for pipeline monitoring," in *Proc. IPSN*, Apr. 2007, pp. 264–273.
- [4] X. Yang *et al.*, "Design of a wireless sensor network for long-term, in situ monitoring of an aqueous environment," *Sensors*, vol. 2, no. 11, pp. 455–472, 2002.
- [5] Y. Yusoff, R. Rosli, M. Karnaluddin, and M. Samad, "Towards smart street lighting system in Malaysia," in *Proc. IEEE ISWTA*, Sep. 2013, pp. 301–305.
- [6] L. Wang, K. Wu, and M. Hamdi, "Combating hidden and exposed terminal problems in wireless networks," *IEEE Trans. Wireless Commun.*, vol. 11, no. 11, pp. 4204–4213, Nov. 2012.
- [7] A. Qayyum, M. Saleem, Tauseef-Ul-Islam, M. Ahmad, and M. Khan, "Performance increase in CSMA/CA with RTS-CTS," in *Proc. 7th INMIC*, Dec. 2003, pp. 182–185.
- [8] T. Suzuki and S. Tasaka, "Performance evaluation of priority-based multimedia transmission with the PCF in an IEEE 802.11 standard wireless LAN," in *Proc. 12th IEEE Int. Symp. PIMRC*, Sep. 2001, vol. 2, pp. G70–G77.
- [9] T. H. Kim and S. Choi, "Priority-based delay mitigation for event-monitoring IEEE 802.15.4 LR-WPANs," *IEEE Commun. Lett.*, vol. 10, no. 3, pp. 213–215, Mar. 2006.
- [10] M. Kim and C.-H. Kang, "Priority-based service-differentiation scheme for IEEE 802.15.4 sensor networks in nonsaturation environments," *IEEE Trans. Veh. Technol.*, vol. 59, no. 7, pp. 3524–3535, Sep. 2010.
- [11] R. Moraes, F. Vasques, P. Portugal, and J. Fonseca, "VTP-CSMA: A virtual token passing approach for real-time communication in IEEE 802.11 wireless networks," *IEEE Trans. Ind. Inf.*, vol. 3, no. 3, pp. 215–224, Aug. 2007.
- [12] H. Zhai and Y. Fang, "A distributed packet concatenation scheme for sensor and ad hoc networks," in *Proc. IEEE MILCOM*, Oct. 2005, pp. 1443–1449.
- [13] G. Bianchi, "Performance analysis of the IEEE 802.11 distributed coordination function," *IEEE J. Sel. Areas Commun.*, vol. 18, no. 3, pp. 535–547, Mar. 2000.
- [14] C. Buratti, "Performance analysis of IEEE 802.15.4 beacon-enabled mode," *IEEE Trans. Veh. Technol.*, vol. 59, no. 4, pp. 2031–2045, May 2010.
- [15] C. Buratti and R. Verdone, "A mathematical model for performance analysis of IEEE 802.15.4 non-beacon enabled mode," in *Proc. Wireless Conf. EW*, Jun. 2008, pp. 1–7.

- [16] N. Abramson, "The ALOHA system—Another alternative for computer communication," in *Proc. AFIPS Comput. Conf.*, vol. 37, 1970, pp. 281–285.
- [17] L. G. Roberts, "ALOHA packet system with and without slots and capture," *ACM SIGCOMM Comput. Commun.*, vol. 5, no. 2, pp. 28–42, Apr. 1975.
- [18] M. Kaynia, G. Oien, and N. Jindal, "Impact of fading on the performance of ALOHA and CSMA," in *Proc. IEEE 10th SPAWC*, Jun. 2009, pp. 394–398.
- [19] A. Hasan and J. G. Andrews, "The guard zone in wireless ad-hoc networks," *IEEE Trans. Wireless Commun.*, vol. 6, no. 3, pp. 897–906, Dec. 2005.
- [20] R. Nelson and L. Kleinrock, "Maximum probability of successful transmission in a random planar packet radio network," in *Proc. IEEE INFOCOM*, Apr. 1983, pp. 365–370.
- [21] F. Baccelli, B. Blaszczyzyn, and P. Muhlethaler, "An ALOHA protocol for multi-hop mobile wireless networks," *IEEE Trans. Inf. Theory*, vol. 52, no. 2, pp. 421–436, Feb. 2006.
- [22] M. Garetto, T. Salonidis, and E. Knightly, "Modeling per-flow throughput and capturing starvation in CSMA multi-hop wireless networks," *IEEE/ACM Trans. Netw.*, vol. 16, no. 4, pp. 864–877, Aug. 2008.
- [23] A. Jindal and K. Psounis, "Making the case for random access scheduling in wireless multi-hop networks," in *Proc. IEEE INFOCOM*, Mar. 2010, pp. 1–5.
- [24] M. Kaynia, P. Nardelli, and M. Latva-aho, "Evaluating the information efficiency of multi-hop networks with carrier sensing capability," in *Proc. IEEE ICC*, Jun. 2011, pp. 1–5.
- [25] P. Jacquet and P. Muhlethaler, "Mean number of transmissions with CSMA in a linear network," in *Proc. IEEE VTC*, Sep. 2010, pp. 1–5.
- [26] P. Muhlethaler and A. Najid, "Throughput optimization of a multi-hop CSMA mobile ad-hoc network," in *Proc. IEEE EW*, Feb. 2004, pp. 1–5.
- [27] A. Busson and G. Chelius, "Point processes for interference modeling in CSMA/CA ad-hoc networks," in *Proc. ACM Int. Symp. PE-WASUN*, Oct. 2009, pp. 1–5.
- [28] N. Tadayon, H. Wang, and H.-H. Chen, "Performance analysis of distributed access multihop Poisson networks," *IEEE Trans. Veh. Technol.*, vol. 63, no. 2, pp. 849–858, Feb. 2014.
- [29] Y. Xiao, "Performance analysis of priority schemes for IEEE 802.11 and IEEE 802.11e wireless LANs," *IEEE Trans. Wireless Commun.*, vol. 4, no. 4, pp. 1506–1515, Jul. 2005.
- [30] S. Jardosh, P. Ranjan, and D. Rawal, "Prioritized IEEE 802.15.4 for wireless sensor networks," in *Proc. WiAD*, Jun. 2010, pp. 1–7.
- [31] H. W. Cho, S. J. Bae, and M. Y. Chung, "Utilization-aware dynamic GTS allocation scheme in IEEE 802.15.4," in *Proc. 16th APCC*, Oct. 2010, pp. 210–214.
- [32] C. Buratti and A. Zanella, "Multihop virtual MIMO systems with channel reuse in a Poisson field of nodes," *IEEE Trans. Veh. Technol.*, vol. 60, no. 5, pp. 2060–2069, Jun. 2011.
- [33] H.-H. Ng, W.-S. Soh, and M. Motani, "On the throughput comparisons of MAC protocols in multi-hop wireless networks," *IEEE Commun. Lett.*, vol. 15, no. 12, pp. 1398–1401, Dec. 2011.
- [34] M. Sikora, J. Laneman, M. Haenggi, J. Costello, and T. Fuja, "Bandwidth- and power-efficient routing in linear wireless networks," *IEEE Trans. Inf. Theory*, vol. 52, no. 6, pp. 2624–2633, Jun. 2006.
- [35] A. Eslami, M. Nekoui, and H. Pishro-Nik, "Results on finite wireless networks on a line," in *Proc. IEEE ITW*, Jan. 2010, pp. 1–5.
- [36] R.-G. Cheng, C.-Y. Wang, L.-H. Liao, and J.-S. Yang, "Ripple: A wireless token-passing protocol for multi-hop wireless mesh networks," *IEEE Commun. Lett.*, vol. 10, no. 2, pp. 123–125, Feb. 2006.
- [37] *Part 15.4: Wireless Medium Access Control (MAC) and Physical Layer (PHY) Specifications for Low-Rate Wireless Personal Area Networks (LR-WPANs)*, IEEE 802.15.4 Std., Piscataway, NJ, USA, 08855-1331: IEEE, 2006.
- [38] C. Buratti and R. Verdone, "P-CSMA: A priority-based CSMA protocol for multi-hop linear wireless networks," in *Proc. 19th EW*, Apr. 2013, pp. 1–8.
- [39] N. Tackett, E. Jovanov, and A. Milenkovic, "An implementation of time synchronization in low-power wireless sensor networks," in *Proc. IEEE 43rd SSST*, Mar. 2011, pp. 61–66.
- [40] C. Buratti and R. Verdone, "Technical Report: L-CSMA—A MAC protocol for multi-hop linear wireless (Sensor) networks." [Online]. Available: http://www.chiaraburatti.org/uploads/TVT_Technical_Report.pdf
- [41] L. Kleinrock, *Queueing Systems*. New York, NY, USA: Wiley, 1975.



Chiara Buratti (M'13) received the M.S. degree in telecommunication engineering and the Ph.D. degree in electronics, computer science and systems from the University of Bologna, Bologna, Italy, in 2003 and 2009, respectively.

She is currently an Assistant Professor with the University of Bologna. She is a coauthor of more than 50 technical papers, most of them IEEE and ACM, and one book. Her research interest is in wireless sensor networks, with particular attention to medium access control and routing protocols, as well

as to the IEEE 802.15.4 standard.



Roberto Verdone (M'13) received the Laurea degree in electronics engineering and the Ph.D. degree from the University of Bologna, Bologna, Italy, in 1991 and 1995, respectively.

Since 2001, he has been a Full Professor in telecommunications with the University of Bologna. He has published more than 100 research papers, mostly in IEEE journals or conferences. His research activity is concerned with both infrastructure-based radio networks and infrastructureless radio networks.

Main topics that he has investigated over the last ten years include radio resource management for cellular systems and medium access control, routing, and topology aspects of wireless sensor networks.